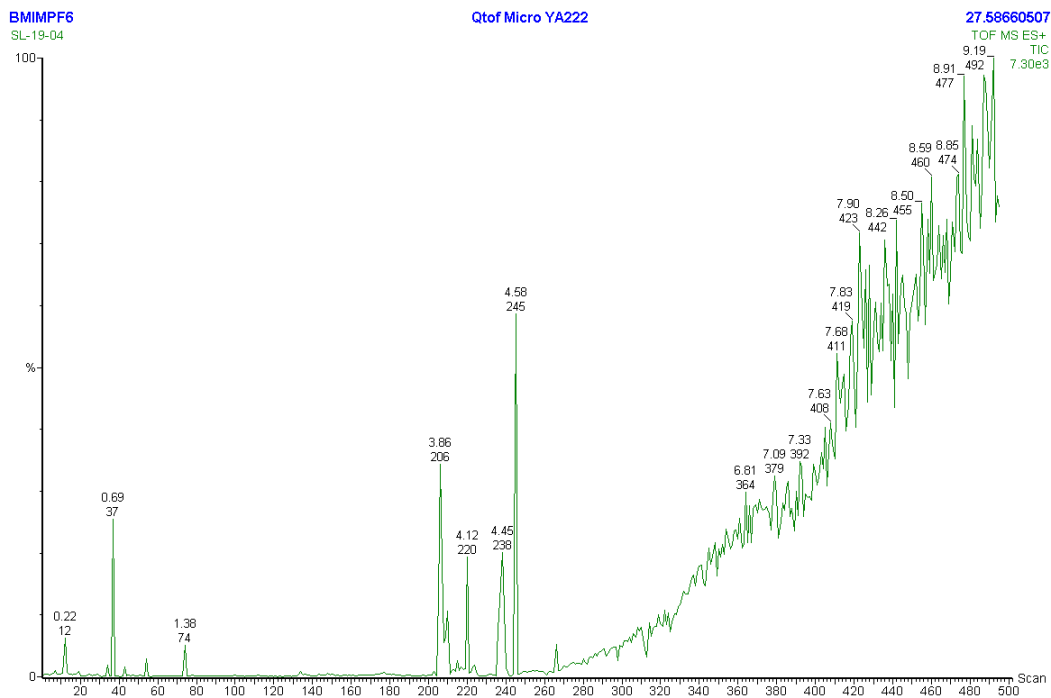
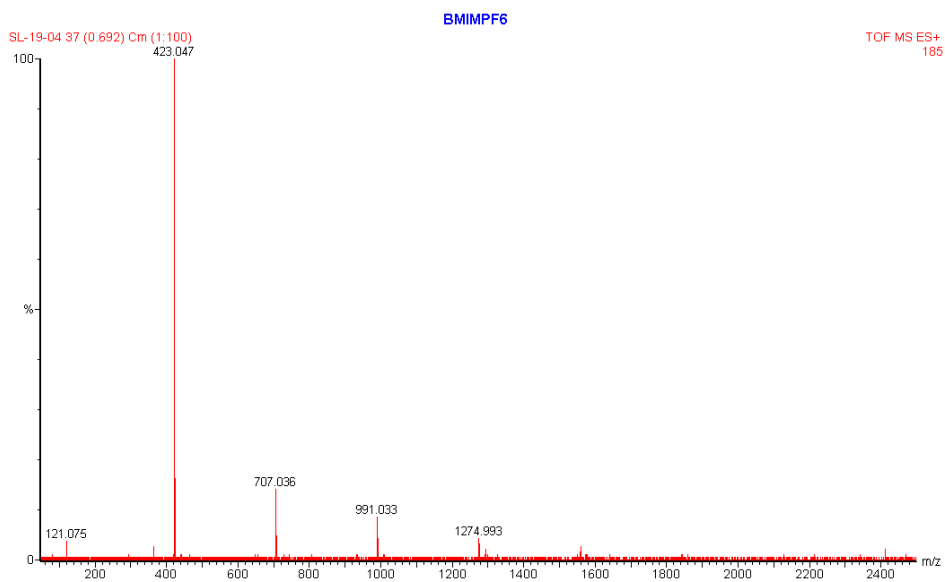


# Other ILs examined by the direct probe approach

[bmim][PF<sub>6</sub>]



**Figure SI.1.** Chromatogram, scan no. approximates T. Note the low abundance of peaks in the low T range (region A), likely due to this IL being particularly free from molecular solvent. Some ion evaporation occurs in region B, and copious decomposition occurs at T above ~300°C.



**Figure SI.2.** Spectrum from region A, showing aggregates of the form [(bmim)<sub>n</sub>(PF<sub>6</sub>)<sub>n-1</sub>]<sup>+</sup>.

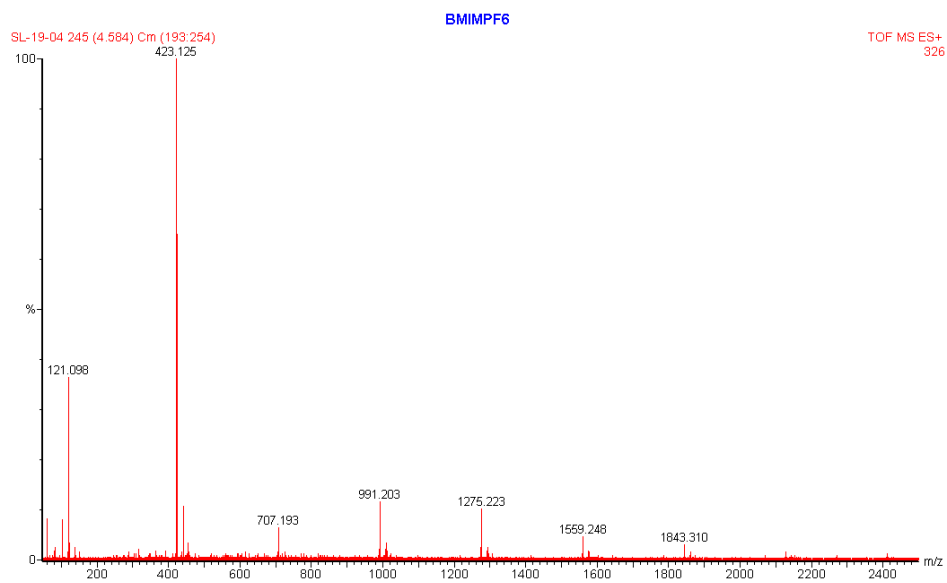


Figure SI.4. Spectrum from region B, showing aggregates of the form  $[(\text{bmim})_n(\text{PF}_6)_{n-1}]^+$ .

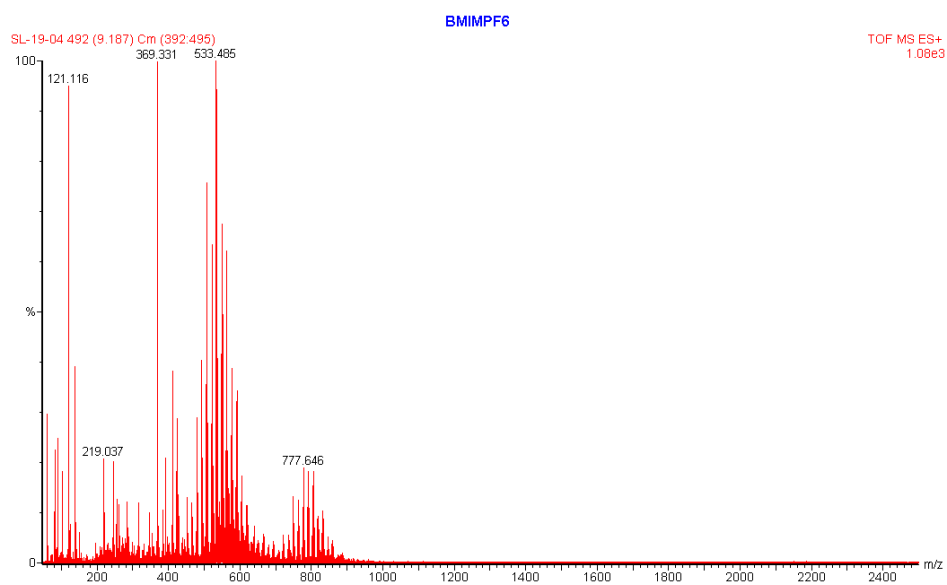
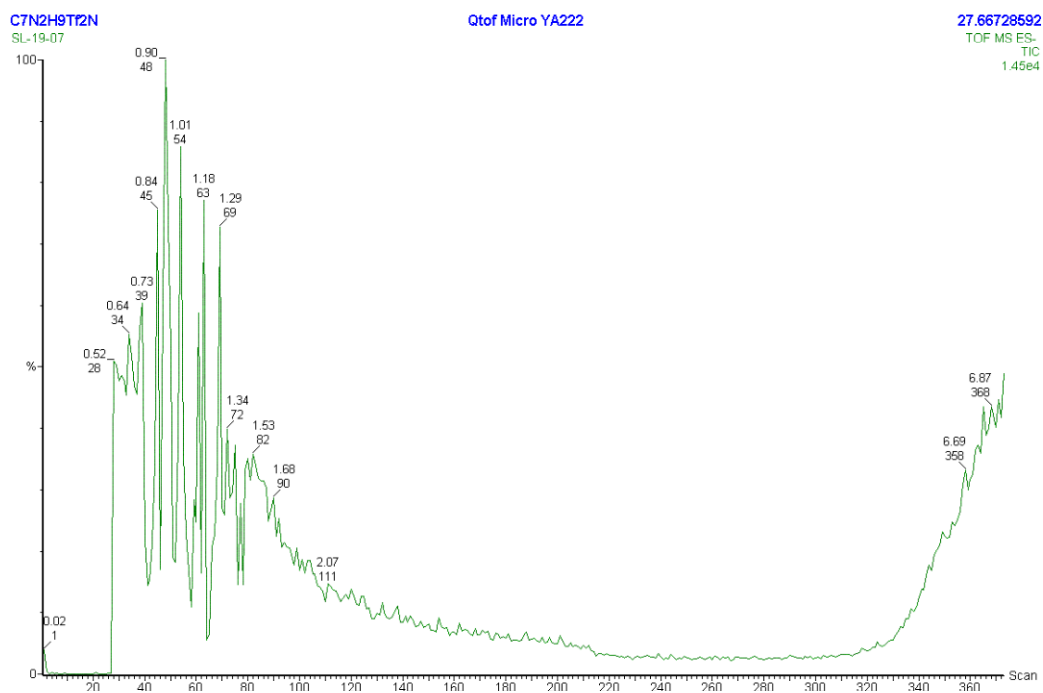
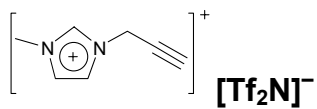
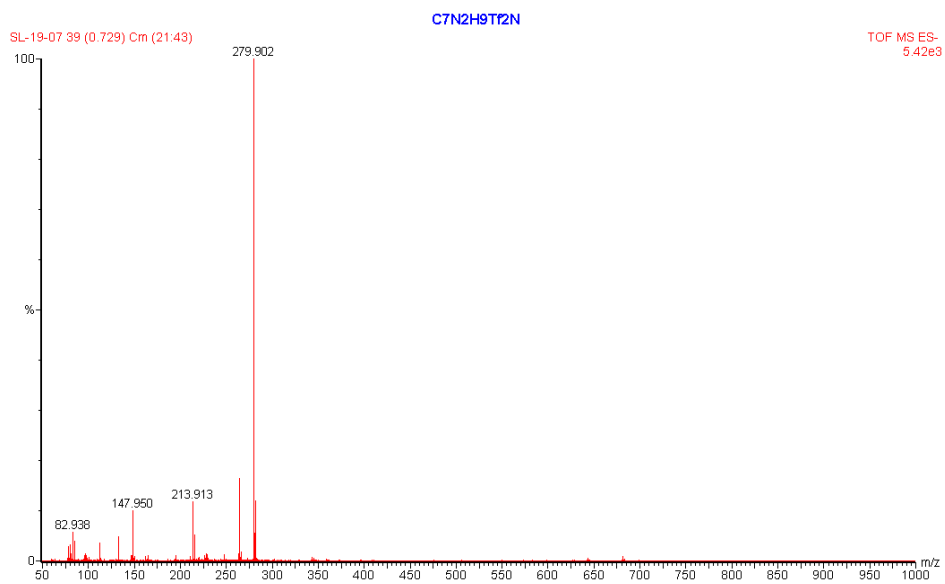


Figure SI.4. Spectrum from region B, showing extensive decomposition products.



**Figure SI.5.** Chromatogram, scan no. approximates T. Note the near-absence of ion current in region B (ion evaporation). Decomposition occurs at T above ~300°C. The negative-ion version showed a similar pattern.



**Figure SI.6.** Negative-ion mass spectrum from region A, showing mostly  $[\text{Tf}_2\text{N}]^-$ .

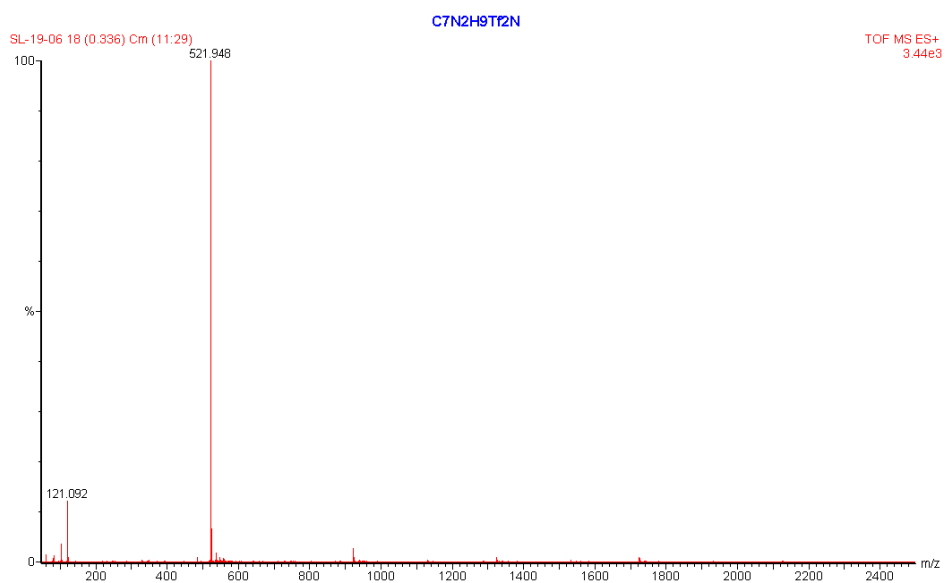


**Figure SI.7.** Positive-ion mass spectrum from region A, showing aggregates of the form  $[(C_7N_2H_9)_n(Tf_2N)_{n-1}]^+$  (though mostly  $[(C_7N_2H_9)_2Tf_2N]^+$ ).

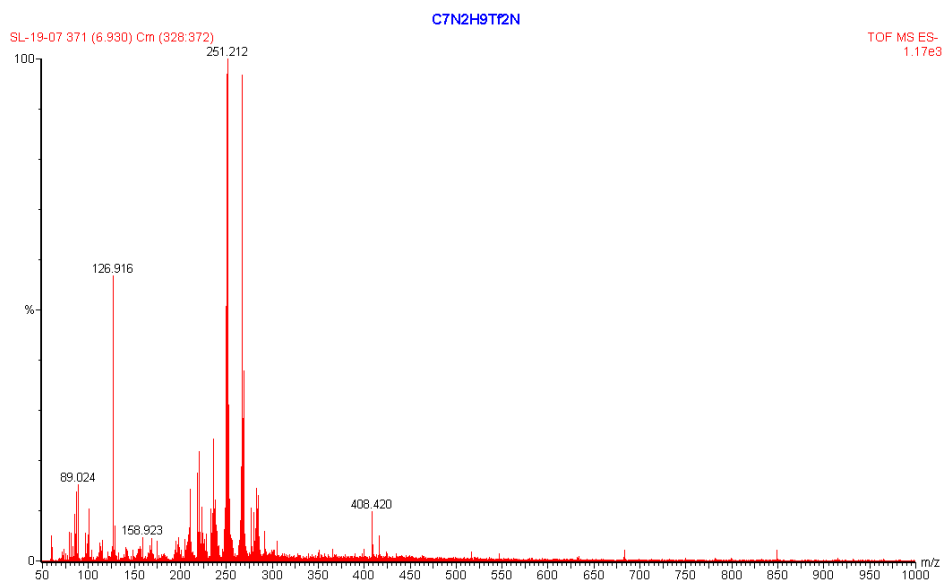


**Figure SI.8.** Negative-ion mass spectrum from region C, showing extensive decomposition products.